Published in the IEEE Transactions on Control of Network Systems, vol. 6, no. 3, pp. 1111-1123, 2019.
doi: 10.1109/TCNS.2019.2921268

On the Need for Communication for Voltage Regulation of Power Distribution Grids

Saverio Bolognani, Ruggero Carli, Guido Cavraro, and Sandro Zampieri

***Abstract*—We consider the problem of regulating the voltage profile of a power distribution grid by controlling the reactive power injection of distributed microgenerators. We define a very general class of purely local feedback controllers in which reactive power injection is adjusted based on the local voltage measurements. This class includes most of the solutions proposed in the literature and in the latest grid code drafts. We show that these strategies do not guarantee the desired regulation, as each of them can have an equilibrium that is not feasible with respect to the desired voltage and power constraints. We then propose a networked feedback law to show that, by adding short-range communication between microgenerators, it is possible to design control strategies that provably converge to the feasible set. This fundamental performance gap between local and networked strategies is finally illustrated via simulations.**

***Index Terms*—Networked control systems, decentralized control, optimization, power distribution, voltage control.**

I. Introduction

FUTURE power distribution grids are expected to host a significant amount of distributed microgeneration and to serve an increasingly higher demand, driven for example by a broader diffusion of electric vehicles. These grids are expected to exhibit congestion phenomena [1]–[4] which cannot be adequately addressed by merely designing oversized networks based on a worst-case analysis (*fit-and-forget*). For example, the voltage profile of these low and medium voltage networks is going to be affected by bidirectional active power flows, and both overvoltage and undervoltage conditions are expected to happen increasingly often.

An avenue that is currently being explored by both researchers and practitioners consists in providing microgenerators with sensing and computation capabilities, and in exploiting the flexibility of their power electronic interface to inject (or withdraw) reactive power from the grid. If properly controlled, these devices can act as a finely distributed network of reactive power compensators, providing a valuable ancillary service to the distribution grid and, ultimately, preventing the curtailment of renewable sources, allowing widespread electric mobility, and postponing grid reinforcement.

S. Bolognani is with the Automatic Control Laboratory, ETH Zurich, 8092 Zurich, Switzerland. Email: bsaverio@ethz.ch.

R. Carli and S. Zampieri are with the Department of Information Engineering, University of Padova, Italy. Email: {carlirug, zampi}@dei.unipd.it.

G. Cavraro is with the National Renewable Energy Laboratory (NREL), Golden, CO, USA. This work was completed before he joined NREL and was not funded by NREL or the US Department of Energy. Email: guido.cavraro@nrel.gov.

This work was supported in part by the European Commission within the Horizon 2020 framework ERIGrid Project under Grant 654113.

Because of the lack of full state monitoring of the distribution grid, most of the efforts towards reactive power control for voltage regulation have focused on purely local (i.e., fully decentralized) feedback strategies (see Figure 1). According to these strategies, the reactive power injection of the power inverter is adjusted based on real-time measurements that can be performed at the point of connection of the power inverter to the grid [5]. Different variations have been proposed (see the review in [6, Section IV.D]). In most cases, the reference for reactive power injection is computed as a static function of the measured voltage amplitude, often with a deadband and/or saturation [7]. Data-driven approaches have been proposed in order to tune these static maps based on past data or prior information on the grid demand and generation [8], [9]. In some strategies, the static feedback is complemented by a feedforward term which is a function of the local active and reactive power demand [10], [11]. An offline optimization of the static feedback (namely of the slope factor and of the thresholds) based on the analysis of the voltage sensitivity matrix, has been suggested in [12].

Since these static feedback laws could lead to oscillatory behaviors, incremental strategies have also been proposed. In this case, the power injection is adjusted based on both the voltage amplitude and the past reactive power setpoint [13], [14]. Other local dynamic controllers have been proposed as well, either by implementing droop-like behaviors that solve some reverse-engineered voltage regulation problems [15], [16] or by explicitly implementing gradient-descent trajectories for the desired cost function [17]–[20]. Different cost functions and different descent methods have been considered, as long as the resulting dynamic update was fully decentralized [21]–[23].

Purely local reactive power control strategies for microgenerators have been considered for inclusion in the latest revisions of some distribution grid codes [24]–[26]. However, it has been empirically observed that these strategies might underperform when compared to "benchmark" solutions, where a centralized controller has access to the entire network state and can optimally dispatch reactive power compensators [27], [28]. Furthermore, even minimal agent-to-agent communication has been shown to be beneficial for this application [29]–[31].

In this paper, we investigate whether there is a *fundamental gap* between the performance of purely local voltage regulation strategies and distributed strategies in which a minimal amount of communication between agents is allowed.

We start by formulating a general class of purely local controllers, which contains the examples mentioned above. The proposed class of controllers has been presented in the preliminary work [32] and includes the smaller class defined

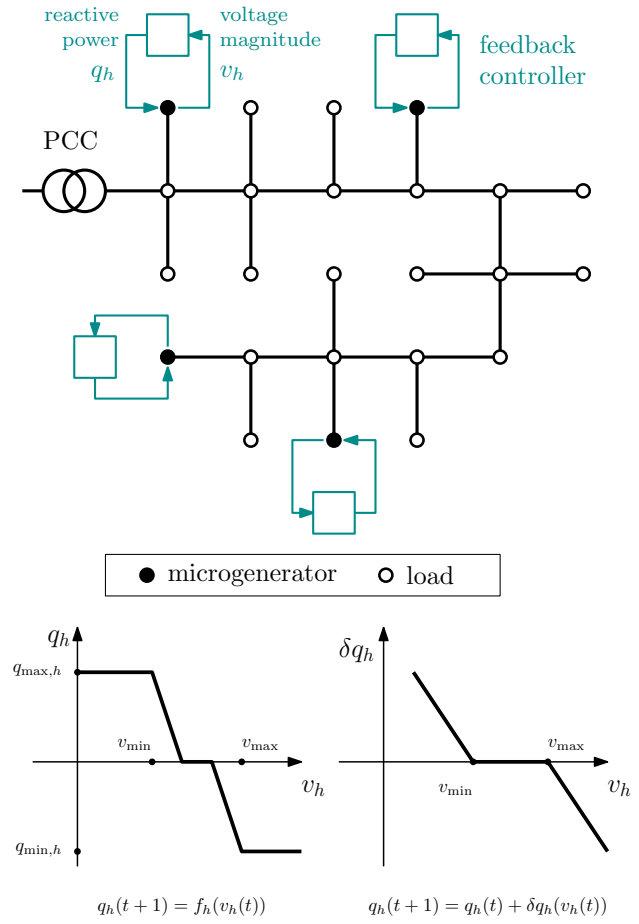

Figure 1. Example of static (left panel) and incremental (right panel) purely local feedback laws for voltage regulation via reactive power injection.

in [33], which only models static maps from the measured voltages to the reactive power control. We show via a counterexample how it is possible to construct scenarios where all these controllers are not effective in regulating the voltage between the desired limits, even if the available reactive power resources would allow it if properly dispatched. In other words, local feedback control laws fail to drive the system to a feasible operating point, despite this being inside the reactive power capability region of the inverters.

Compared to [32], in this paper we complete the investigation of this fundamental performance gap by presenting a distributed reactive power control strategy which requires only short-range communications, uses the same measurements available for the local control strategies (voltage magnitudes at the microgenerators and no phasor measurement), does not require monitoring of all buses (in contrast to the distributed solutions in [34]–[38]), and provably converges to a feasible operating point that guarantees satisfaction of the grid voltage limits. From an application perspective, this Volt/VAR strategy is interesting *per se*: to the best of our knowledge, no coordinated voltage regulation strategy available in the literature meets these specifications (except for the working paper [39], based on a different iterative optimization method).

We illustrate these results in simulation on the IEEE 123-bus feeder, using real power consumption and generation data.

All the proofs are collected in the Appendix.

A. Mathematical notation

We define by $\mathbf{1}$ the column vector of all ones, while e_v is the vector whose value is 1 in position v, and 0 elsewhere.

Given $u, v, w \in \mathbb{R}^\ell$, with $v_h \leq w_h, h = 1, \dots, \ell$ we define the operator $[u]_v^w$ as the component wise projection of u in the set $\left\{x \in \mathbb{R}^\ell : v_h \leq x_h \leq w_h, h = 1, \dots, \ell\right\}$, that is,

$$([u]_v^w)_h = \begin{cases} u_h & \text{if } v_h \leq u_h \leq w_h \\ v_h & \text{if } u_h < v_h \\ w_h & \text{if } u_h > w_h \end{cases} \tag{1}$$

Finally, we denote by $\overline{u}$, $\operatorname{Re} u$, and $\operatorname{Im} u$, the complex conjugate, the real part, and the imaginary part of u, respectively.

II. Power distribution grid model

We consider a grid-connected, balanced, power distribution network, on which we define the following steady state quantities for each bus $h \in \mathcal{V} := \{1, \dots, n\}$:

- v_h voltage magnitudes
- θ_h voltage angles
- p_h active power injections
- q_h reactive power injections

We then define v (and similarly θ, p, q) as the vectors containing all the scalar quantities v_h (respectively θ_h, p_h, q_h).

All power flows that are compatible with the physics of the grid (namely with Kirchhoff's and Ohm's law) must satisfy the nonlinear complex-valued equation

$$\operatorname{diag}(u)\overline{Yu} = s \tag{2}$$

where $u_h = v_h e^{j\theta_h}$ and $s_h = p_h + jq_h$ denote the complex bus voltages and complex bus power injections, respectively, and where Y is the bus admittance matrix of the grid. We neglect shunt admittances and therefore assume $Y\mathbf{1} = 0$.

We label the substation (where the distribution grid connects to the higher voltage grid) as node 1 and consider it as an ideal sinusoidal voltage generator (*slack bus*) at the nominal voltage $v_1 = 1$, with arbitrary, but fixed, angle θ_1. We model all nodes except the substation as *constant power buses*. These include both loads and microgenerators.

We adopt a linearized model to express the relation between voltages and nodal powers in the grid. The linearization of the power flow equations around a flat voltage profile yields the implicit relation [40]

$$\begin{bmatrix} \operatorname{Re} Y & -\operatorname{Im} Y \\ -\operatorname{Im} Y & -\operatorname{Re} Y \end{bmatrix} \begin{bmatrix} v \\ \theta \end{bmatrix} \approx \begin{bmatrix} p \\ q \end{bmatrix}, \tag{3}$$

which is a good approximation when $v \approx \mathbf{1}$ and $\theta, p, q \approx 0$.

It can be shown [29, Lemma 1] that there exists a unique symmetric, positive semidefinite matrix $X \in \mathbb{C}^{n \times n}$ such that

$$\begin{cases} YX = I - e_1\mathbf{1}^\intercal \\ Xe_1 = 0, \end{cases} \tag{4}$$

which depends only on the topology of the grid power lines and on their impedances, and whose elements are all non-negative. This matrix allows to derive the following convenient explicit expression for the voltage magnitudes.

Lemma 1. *Let Y be a bus admittance matrix satisfying $Y\mathbf{1} = 0$, and let X be defined as in* (4)*. Then, when $p, q \approx 0$,*

$$v \approx \mathbf{1} + \operatorname{Re} Xp + \operatorname{Im} Xq. \tag{5}$$

Equation (5) models the well known fact that the injection or the absorption of reactive power increase or decrease, respectively, the voltage magnitude also in the case of not purely inductive lines. Notice in fact that we have made no assumption on the X/R ratio of the lines.

The quality of this linearization can be studied following the analysis in [41], and relies on having large nominal voltage of the grid and relatively small nodal currents. This assumption is verified in practice, and corresponds to correct design and operation of distribution networks, where indeed the nominal voltage is chosen sufficiently large in order to deliver power to the loads with relatively small power losses.

Finally, we assume that microgenerators are connected to a subset of the grid buses, namely $\mathcal{C} \subseteq \mathcal{V}$ (with $|\mathcal{C}| = m$). As in Figure 1, each microgenerator is provided with

- *sensing capabilities*, so that it can take local voltage magnitude measurements;
- *computational capabilities* that will be exploited to implement the control algorithms;
- *actuation capabilities*, being able to regulate the amount of reactive power injected into the grid.

In order to underline the difference among microgenerators and passive loads in the notation, we introduce the following block decomposition of the voltage magnitude vector v

$$v = \begin{bmatrix} v_1 \\ v_G \\ v_L \end{bmatrix}, \tag{6}$$

where v_1 is the voltage magnitude at the substation, $v_G \in \mathbb{R}^m$ are the voltage magnitudes at the microgenerators, and $v_L \in \mathbb{R}^{n-m-1}$ are the voltage magnitudes at the loads. Similarly, we also define $s_G = p_G + jq_G$ and $s_L = p_L + jq_L$. Accordingly with the same partitioning, we can partition the matrix X as

$$\begin{bmatrix} 0 & 0 & 0 \\ 0 & X_{GG} & X_{GL} \\ 0 & X_{LG} & X_{LL} \end{bmatrix}.$$

The structure of X descends from the property of the Green's matrix, and the block X_{GG} is invertible [18].

With this decomposition, we then have

$$v_G \approx \mathbf{1} + X^R_{GG} p_G + X^R_{GL} p_L + X^I_{GG} q_G + X^I_{GL} q_L, \tag{7}$$

where the superscripts R and I indicate the real and imaginary part of the block, respectively. In the sequel for simplicity we will use (7) as an equality, even if it provides only an approximate relation between the quantities on the model.

III. Voltage control via reactive power regulation

In this section, we formulate the problem of controlling the reactive power injected (or withdrawn) by the microgenerators in order to regulate the voltage profile of the distribution feeder. Since we assume that only microgenerators can measure their bus voltage, we consider the constraints

$$v_{\min} \le v_h \le v_{\max}, \qquad \forall\ h \in \mathcal{C}, \tag{8}$$

where $v_{\min}$ and $v_{\max}$ are, respectively, the minimum and maximum admissible values for the voltage magnitudes. Typical scenarios include both symmetric bounds around the nominal voltage (e.g. $\pm 10\%$) and asymmetric bounds (e.g. $v_{\min} = 0.87, v_{\max} = 1.06$).

In addition, since the generators deployed in the distribution network are, typically, of small size, we need to take into account also constraints on their generation capabilities. Precisely, we assume that

$$q_{\min,h} \le q_h \le q_{\max,h}, \qquad \forall\ h \in \mathcal{C}, \tag{9}$$

where $q_{\min,h}$, $q_{\max,h}$ denote, respectively, the minimum and the maximum amount of reactive power that can be injected by agent h. In most cases $q_{\min,h} \le 0$ and $q_{\max,h} \ge 0$.

Based on the constraints in (8) and in (9), we introduce a proper definition of the set of the *feasible reactive power injections*. Observe that, in the setup we consider, the quantities p_G, p_L and q_L are assumed to be constant and that only q_G is actuated in order to regulate v_G; in other words, v_G can be described as a function of q_G via (7). A given q_G is said to be feasible if it satisfies (9) and if the induced $v_G(q_G)$ satisfies (8). More formally, for a given triple (p_G, p_L, q_L), we define

$$\mathcal{F}(p_G, p_L, q_L) = \big\{ q_G \text{ such that } \forall h \in \mathcal{C} \text{ it holds } q_{\min,h} \le q_h \le q_{\max,h}, v_{\min} \le v_h \le v_{\max} \big\}. \tag{10}$$

Since there is no risk of confusion, for the sake of notational convenience, we omit the dependence of $\mathcal{F}$ on (p_G, p_L, q_L).

The goal of a reactive power control strategy is to drive the reactive power injection of the microgenerators to a point that belongs to the set $\mathcal{F}$, for any initial condition.

In all the strategies that we consider in this paper, microgenerators measure periodically and synchronously the magnitudes of their voltages; namely, all the agents take their measurements at time instants $t = 0, 1, \ldots$ where without loss of generality we have assumed unitary sampling time. Based on those measurements, they synchronously update their reactive power injection, and hold the same value until the next measurement.

IV. A class of purely local control strategies

In this section, we define a family of *purely local* strategies, in which each agent h updates q_h based only on its current reactive power injection and on the measurements of the magnitude of its own voltage, i.e., v_h; in these strategies, agents do not communicate with each other. The family we introduce includes most of the purely local strategies that have been recently proposed in the literature and in the latest grid code drafts, as reviewed in the Introduction.

In these strategies, the reactive power output of each microgenerator $h \in \mathcal{C}$ can be expressed as

$$q_h(t+1) = g_h(q_h(t), v_h(t)). \tag{11}$$

We will say that a controller

$$g_h : [q_{\min,h}, q_{\max,h}] \times \mathbb{R}_{\geq 0} \to [q_{\min,h}, q_{\max,h}]$$

belongs to the class $\mathcal{G}$ if it meets the following properties:

1) the function $g_h(q, \cdot)$ is continuous $\forall q \in [q_{\min,h}, q_{\max,h}]$;
2) the function $g_h(\cdot, v)$ satisfies

$$g_h(q, v) - g_h(q', v) < q - q'; \tag{12}$$

for every $q, q' \in [q_{\min,h}, q_{\max,h}]$, with $q > q'$;

3) the function $g_h(q, \cdot)$ is weakly decreasing, i.e. for every $0 \leq v \leq v'$,

$$g_h(q, v) \geq g_h(q, v'). \tag{13}$$

According with the principle that the local voltage is an increasing function of the reactive power injection, condition 3) states that the lower the actual voltage is, the higher the reactive power output will be. Conditions 1) and 2) are instead typically introduced to obtain a stable dynamic behavior of the closed-loop system.

Remark 1. $\mathcal{G}$ is a wide class, containing several algorithms proposed in the literature. For instance, all the strategies in which the power injection is computed as a static function of the measured voltage amplitude, i.e. those that can be expressed as

$$g_h(q, v) = f_h(v) \tag{14}$$

where $f_h(v)$ is a function of the type depicted in the left panel of Figure 1, fit in $\mathcal{G}$. As reviewed in the Introduction, the formulation (14) describes a large number of proposed control strategies. Furthermore, also the *incremental* versions of (14), whose update rules are either

$$g_h(q, v) = [q + \gamma(f_h(v) - q)]_{q_{\min,h}}^{q_{\max,h}} \tag{15}$$

or

$$g_h(q, v) = [q + \gamma(f_h^{-1}(q) - v)]_{q_{\min,h}}^{q_{\max,h}} \tag{16}$$

(presented respectively in [13] and [14]), belong to $\mathcal{G}$.

A configuration (q_h^*, v_h^*) is said to be an equilibrium for the algorithms g_h if it satisfies the equation

$$q_h^* = g_h(q_h^*, v_h^*). \tag{17}$$

The equilibria of the algorithms in $\mathcal{G}$ have a notable feature: the reactive power output of each agent can be exactly inferred from the knowledge of its equilibrium voltage, as the following result shows.

Proposition 2. *Let $g_h(q, v)$ belong to $\mathcal{G}$. Given $v^* \in \mathbb{R}_{\geq 0}$, there exists only one q^* such that equation* (17) *holds.*

Thanks to Proposition 2, we can define, for each agent h, the *equilibrium function*

$$\begin{aligned} F_h : \mathbb{R}_{\geq 0} &\to [q_{\min,h}, q_{\max,h}] \\ v &\mapsto q : q = g_h(q, v) \end{aligned}$$

which, given the equilibrium voltage of agent h, returns its reactive power output.

The next proposition studies some properties of the equilibrium function.

Proposition 3. *Let $F_h(v)$ be the equilibrium function associated with the controller $g_h(q, v) \in \mathcal{G}$. Then $F_h(v)$ is continuous and weakly decreasing.*

Remark 2. For the particular local control strategies described by the update laws (14), (15), (16), it can be easily shown that the equilibrium function is

$$F_h(v) = f_h(v).$$

In addition, it is worth mentioning that there are strategies that do not fit in $\mathcal{G}$, for instance the local control law proposed in [21], which can be expressed in the form

$$g_h(q, v) = [q + f_h(v)]_{q_{\min,h}}^{q_{\max,h}}. \tag{18}$$

This incremental control law belongs to a more general class composed by controllers that, instead of (12), satisfy

$$g_h(q, v) - g_h(q', v) \leq q - q'.$$

The difficulty in this case is that the equilibrium function is a *set valued function* i.e., given a value of v, there is set of reactive power output for which equation (17) holds. We will specifically comment on this incremental control law in the numerical analysis of Section VI.

So far, we characterized the equilibria of a single controller. There remains the open question of what happens when every agent in a smart distribution grid is commanded by a local controller belonging to $\mathcal{G}$.

Let us define the function

$$\begin{aligned} F(\cdot) : \mathbb{R}_{\geq 0}^m &\to [q_{\min,1}, q_{\max,1}] \times \cdots \times [q_{\min,m}, q_{\max,m}] \\ [F(v)]_h &= F_h(v). \end{aligned}$$

$F(\cdot)$ is a diagonal map with entries that are weakly decreasing.

In principle there could exist one, many or even zero solutions of the power flow equations (2) coupled with the equilibrium equations of the local controllers $q_G = F(v_G)$. We are able to discuss the existence and uniqueness of solutions if the power flow equations (2) are in the linear regime, namely when p_G, p_L, q_G, q_L are small. In this case, (q_G, v_G) is an equilibrium if and only if it solves the system of equations

$$\begin{aligned} q_G &= F(v_G) \\ v_G &= \mathbf{1} + X_{GG}^I q_G + b \end{aligned}$$

where

$$b := X_{GG}^R p_G + X_{GL}^R p_L + X_{GL}^I q_L.$$

If we let $\delta_{v_G} := v_G - \mathbf{1}$ we can find equivalently that

$$\delta_{v_G} = X_{GG}^I F(\mathbf{1} + \delta_{v_G}) + b. \tag{19}$$

Since X_{GG}^I is positive definite we can write

$$(X_{GG}^I)^{-1} \delta_{v_G} - F(\mathbf{1} + \delta_{v_G}) = (X_{GG}^I)^{-1} b,$$

where $(X_{GG}^I)^{-1}$ is positive definite as well. We are in a position to apply the result in [42] and prove that, for any b, equation (19) has a unique solution in δ_{v_G}. Since the linear approximation is valid only locally, what we found is true only if both b and δ_{v_G} are close to zero.

Now that we have introduced a well defined function F that maps voltage profiles v_G into equilibrium reactive power injections q_G, we can discuss the effectiveness of this class of local strategies for the regulation of the voltage.

In the rest of this section we provide a simple counterexample in which, for any controller in $\mathcal{G}$, there exists an equilibrium of the algorithm that does not belong to $\mathcal{F}$ (i.e., it is not feasible), even if $\mathcal{F} \neq \emptyset$ (i.e., a feasible reactive power injection exists).

A. A simple example of the ineffectiveness of local strategies

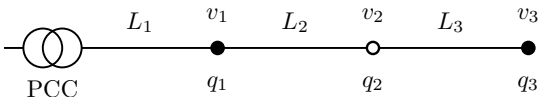

Consider a network composed of four nodes (the substation, a microgenerator, a load, and another microgenerator) connected forming a line, as in figure, via inductances L_1, L_2, and L_3. We assume, for ease of notation, that $v_{\min} = 1-\delta$ and $v_{\max} = 1+\delta$, for a given $\delta > 0$. With no loss of generality, we assume that, when $v_1 = 1$, $F_1(1) = \bar{q}_1 \in [q_{\min,1}, q_{\max,1})$. We aim at showing that, for any value of L_1, L_2, and L_3 there exist values of $q_{\max,3}$ and q_2 such that

i) all local algorithms of the class $\mathcal{G}$ have an unfeasible equilibrium $(q_1^*, q_3^*) \notin \mathcal{F}$;
ii) there exists a feasible reactive power injection ($\mathcal{F} \neq \emptyset$).

As all lines are purely inductive and the voltage at the substation is 1, the linearized model gives

$$v_1 = 1 + L_1 q_1 + L_1 q_2 + L_1 q_3$$
$$v_3 = 1 + L_1 q_1 + (L_1 + L_2) q_2 + (L_1 + L_2 + L_3) q_3.$$

We know that, for any value of q_2, an equilibrium (q_1^*, v_1^*), (q_3^*, v_3^*) exists. We first show that, if

$$q_2 = Q := -\frac{1}{L_2}\delta - \frac{L_2 + L_3}{L_2} q_{\max,3}, \tag{20}$$

then $v_3^* < 1 - \delta$. In order to do so, observe that

$$\begin{aligned} v_1^* - v_3^* &= -L_2 q_2 - (L_2 + L_3) q_3^* \\ &\geq -L_2 Q - (L_2 + L_3) q_{\max,3} = \delta. \end{aligned}$$

Observe moreover that, if we define $\phi_1(v_1) := v_1 - 1 - L_1 F_1(v_1)$, then

$$\begin{aligned} \phi_1(v_1^*) &= L_1 q_2 + L_1 q_3^* \\ &\leq L_1 Q + L_1 q_{\max,3} = -\frac{L_1}{L_2}\delta - \frac{L_1 L_3}{L_2} q_{\max,3}. \end{aligned}$$

Since $\phi_1(v_1)$ is strictly increasing and $\phi_1(1) = -L_1 F_1(1) = -L_1 \bar{q}_1$, we can argue that if

$$\frac{1}{L_2}\delta + \frac{L_3}{L_2} q_{\max,3} > \bar{q}_1 \tag{21}$$

then $v_1^* < 1$ which, together with the fact that $v_1^* - v_3^* \geq \delta$ yields $v_3^* < 1 - \delta$.

This proves that if $q_2 = Q$ (and, in fact, if $q_2 \leq Q$), then the equilibrium is not feasible.

In order to complete the example we show under which conditions there exist reactive powers $q_1 \in [q_{\min,1}, q_{\max,1}]$, $q_3 \in [q_{\min,3}, q_{\max,3}]$ such that $v_1, v_3 \in [1-\delta, 1+\delta]$, when $q_2 = Q$. Let us take $q_3 = q_{\max,3}$. Then

$$v_1 = 1 + L_1 q_1 - \frac{L_1 L_3}{L_2} q_{\max,3} - \frac{L_1}{L_2}\delta$$
$$v_3 = 1 + L_1 q_1 - \frac{L_1 L_3}{L_2} q_{\max,3} - \frac{L_1 + L_2}{L_2}\delta = v_1 - \delta$$

From this we can argue that the state is feasible if and only if q_1 is such that $v_1 \in [1, 1+\delta]$. This condition is equivalent to the fact that

$$\frac{1}{L_2}\delta + \frac{L_3}{L_2} q_{\max,3} \leq q_1 \leq \frac{1}{L_2}\delta + \frac{L_3}{L_2} q_{\max,3} + \frac{1}{L_1}\delta.$$

We can conclude that there exists $q_1 \in [q_{\min,1}, q_{\max,1}]$ such that the previous inequality holds if and only if

$$\frac{1}{L_2}\delta + \frac{L_3}{L_2} q_{\max,3} \leq q_{\max,1} \tag{22}$$
$$\frac{1}{L_2}\delta + \frac{L_3}{L_2} q_{\max,3} \geq q_{\min,1} - \frac{1}{L_1}\delta. \tag{23}$$

Notice that (23) is automatically satisfied if (21) is satisfied. It is therefore enough to choose q_2 according to (20) and $q_{\max,3}$ according to (21) and (22) in order to obtain the desired counterexample that is valid for *all* strategies belonging to the class of local strategies $\mathcal{G}$.

V. A NETWORKED CONTROL STRATEGY

After having assessed the limitations of purely local strategies in Section IV, we now investigate whether communication between compensators allows to design a feedback control law that is guaranteed to converge to the region $\mathcal{F}$ where both voltage and reactive power constraints are satisfied. In order to derive a sharp characterization of the *minimal* communication that is needed to successfully solve the voltage regulation problem, we only allow short-range communication between the microgenerators. More precisely, we derive a distributed voltage control strategy (denoted hereafter as DVS) in which every agent $h \in \mathcal{C}$ can communicate with its neighbors, defined as follows.

Definition 4 (Neighbor microgenerators)**.** *Let $h \in \mathcal{C}$ be a microgenerator. The set of neighbors of h, denoted as $\mathcal{N}(h)$, is the subset of $\mathcal{C}$ defined as*

$$\mathcal{N}(h) = \{k \in \mathcal{C} \mid \exists\, \pi \in \mathcal{P}_{hk}, \pi \cap \mathcal{C} = \{h, k\}\},$$

where $\mathcal{P}_{hk}$ is the set of paths going from bus h to bus k..

See Figure 2 for an example, and notice that $h \in \mathcal{N}(h)$.

In the following, we illustrate the design process that yields this networked control strategy and we then detail all the operations that need to be performed by the agents.

We start by reformulating the voltage regulation specifications introduced in Section III as a constrained optimization problem

$$\min_{q_G} \quad \frac{1}{2} q_G^T X_{GG}^I q_G \tag{24a}$$
$$\text{subject to} \quad \begin{array}{l} v_{\min} \leq v_h(q_G) \leq v_{\max} \\ q_{\min,h} \leq q_h \leq q_{\max,h} \end{array} \quad \forall h \in \mathcal{C} \tag{24b}$$

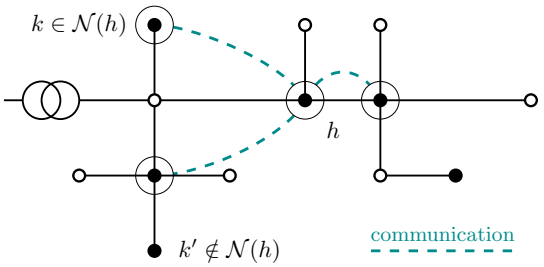

Figure 2. An example of neighbor microgenerators. Black nodes are microgenerators ($h \in \mathcal{C}$). White nodes are loads. The circled microgenerators belong to the set $\mathcal{N}(h)$ of neighbors of h. For each agent $k \in \mathcal{N}(h)$, the path that connects h to k does not include any other microgenerator.

where $v_h(q_G)$ represents the h-th element of the right hand side of (7). The feasible region of (24) corresponds exactly to the set $\mathcal{F}$ defined in (10), and therefore the two representations are completely equivalent.

Remark 3. For the sake of consistency with the specifications of the fully decentralized problem, (24) only includes voltage constraints on the buses that host a microgenerator. This formulation can be easily generalized: if the voltage at a load bus h' can be measured, and this measurement can be communicated, then the corresponding voltage limits can be included in the optimization problem by adding a fictitious generator at that bus with $q_{\min,h'} = q_{\max,h'}$.

We now derive an iterative algorithm for the solution of (24), whose iterative steps will ultimately correspond to the feedback law of our DVS. We start by dualizing the voltage constraints in (24b). We therefore introduce, for each agent $h \in \mathcal{C}$, the Lagrange multipliers $\lambda_{\min,h}$ and $\lambda_{\max,h}$ corresponding to the constraints $v_h \geq v_{\min}$, $v_h \leq v_{\max}$, respectively. For ease of notation, we indicate by λ the vector of all these multipliers. The resulting partial Lagrangian is

$$\boldsymbol{L}(q_G, \lambda) = \frac{1}{2} q_G^T X_{GG}^I q_G + \sum_{h \in \mathcal{C}} \lambda_{\min,h} \left(v_{\min} - v_h(q_G)\right) + \sum_{h \in \mathcal{C}} \lambda_{\max,h} \left(v_h(q_G) - v_{\max}\right).$$

The corresponding dual function becomes

$$g(\lambda) = \min_{q_G} \left\{ \boldsymbol{L}(q_G, \lambda) \mid q_{\min,h} \leq q_h \leq q_{\max,h} \ \forall h \in \mathcal{C} \right\}, \tag{25}$$

which can be maximized by employing a subgradient ascent algorithm on the dual variables $\lambda_{\min,h}$ and $\lambda_{\max,h}$. A subgradient for the dual $g(\lambda)$ is given by the violation of the dualized constraints at the solution q_G^* of the minimization problem in (25), i.e.,

$$v_{\min} - v_h(q_G^*) \in \partial_{\lambda_{\min,h}} g(\lambda)$$
$$v_h(q_G^*) - v_{\max} \in \partial_{\lambda_{\max,h}} g(\lambda).$$

The term $v_h(q_G^*)$ that appears in all these subgradients does not have to be explicitly computed (which would require to know the entire grid model). It can be measured directly by agent h, if the reactive power injection of the compensators corresponds to q_G^*.

For the solution of the inner constrained optimization problem (25), we again apply dual decomposition, this time with respect to the constraints on the reactive power injections q_h. We therefore introduce the Lagrange multipliers $\mu_{\min,h}$ and $\mu_{\max,h}$, corresponding to the constraints $q_h \geq q_{\min,h}$ and $q_h \leq q_{\max,h}$, respectively. As before, we denote by μ the vector containing all these multipliers. The resulting Lagrangian is

$$\boldsymbol{L}_\lambda(q_G, \mu) = \boldsymbol{L}(q_G, \lambda) + \sum_{h \in \mathcal{C}} \mu_{\min,h} \left(q_{\min,h} - q_h\right) + \sum_{h \in \mathcal{C}} \mu_{\max,h} \left(q_h - q_{\max,h}\right).$$

For the solution of this optimization subproblem, we propose to alternate again an exact minimization step in the primal variables q_G, i.e.,

$$g_\lambda(\mu) = \min_{q_G} \boldsymbol{L}_\lambda(q_G, \mu), \tag{26}$$

and a subgradient ascent step in the dual variables μ. Notice that, differently from before, the primal step (26) is an unconstrained quadratic program, for which we derive a closed-form solution. Moreover, the subgradients

$$q_{\min,h} - \hat{q}_h \in \partial_{\mu_{\min,h}} g_\lambda(\mu)$$
$$\hat{q}_h - q_{\max,h} \in \partial_{\mu_{\max,h}} g_\lambda(\mu)$$

can be directly evaluated in the algorithm based on the solution $\hat{q}$ of the minimization in (26).

A. Description of the control algorithm

Inspired by the iterative optimization algorithm that we described, we propose the following feedback control law. It is composed of two feedback loops that are executed at different sample rates: one at times $t = 0, 1, 2, \ldots$ and another one at times $\tau = 0, \frac{1}{K}, \frac{2}{K}, \ldots$, where K is a positive integer.

At any time t each agent $h \in \mathcal{C}$ has in its memory the value of the variables $\lambda_{\min,h}(t), \lambda_{\max,h}(t)$, $\mu_{\min,h}(t), \mu_{\min,h}(t)$, $\hat{q}_h(t)$, and it executes the following actions.

1) It executes the following K iterations at times $\tau = t, t + \frac{1}{K}, t + \frac{2}{K}, \ldots, t + \frac{K-1}{K}$:

1.1) it updates the variables $\mu_{\min,h}, \mu_{\max,h}$ as

$$\mu_{\min,h}\left(\tau + \tfrac{1}{K}\right) = \left[\mu_{\min,h}(\tau) + \gamma\left(q_{\min} - \hat{q}_h(\tau)\right)\right]_0^\infty$$
$$\mu_{\max,h}\left(\tau + \tfrac{1}{K}\right) = \left[\mu_{\max,h}(\tau) + \gamma\left(\hat{q}_h(\tau) - q_{\max}\right)\right]_0^\infty$$

where γ is a positive constant;

1.2) it gathers the values of the variables

$$\mu_{\min,k}\left(\tau + \tfrac{1}{K}\right), \ \mu_{\max,k}\left(\tau + \tfrac{1}{K}\right), \quad k \in \mathcal{N}(h)$$

from its neighbors;

1.3) it updates the variable $\hat{q}_h$ as

$$\hat{q}_h\left(\tau + \tfrac{1}{K}\right) = \lambda_{\min,h}(t) - \lambda_{\max,h}(t) + \sum_{k \in \mathcal{N}(h)} G_{hk}\left(\mu_{\min,k}\left(\tau + \tfrac{1}{K}\right) - \mu_{\max,k}\left(\tau + \tfrac{1}{K}\right)\right) \tag{27}$$

where G_{hk} are the elements of the inverse of X_{GG}^I.

At the end of these K iterations, agent h has computed the value of the variables $\mu_{\min,h}(t+1), \mu_{\min,h}(t+1), \hat{q}_h(t+1)$.
2) It measures its voltage magnitude $v_h(t+1)$.
3) It updates the variables $\lambda_{\min,h}, \lambda_{\max,h}$ as

$$\lambda_{\min,h}(t+1) = [\lambda_{\min,h}(t) + \alpha\,(v_{\min} - v_h(t+1))]_0^{\infty}$$
$$\lambda_{\max,h}(t+1) = [\lambda_{\max,h}(t) + \alpha\,(v_h(t+1) - v_{\max})]_0^{\infty}$$

where α is a positive constant.
4) It adjusts the amount of injected reactive power q_h to the value obtained by projecting the internal variable $\hat{q}_h$ into the feasible set defined by (9), i.e.,

$$q_h(t+1) = [\hat{q}_h(t+1)]_{q_{\min,h}}^{q_{\max,h}}. \tag{28}$$

Observe that steps 2), 3), and 4) are completely local. In order to perform step 1) each agent needs to gather information only from its neighbors. Moreover, they need to know only local electrical parameters of the grid via the elements of G, as shown in the following lemma (which can be proved following the steps in [30, Appendix A]).

Lemma 5. *The inverse G of X_{GG}^I has the sparsity pattern induced by the Definition 4 of neighbor microgenerators, i.e.*

$$G_{hk} \neq 0 \quad \Leftrightarrow \quad k \in \mathcal{N}(h).$$

Moreover, the value of each element G_{hk} depends only on the line impedances connecting h and k to their neighbors.

Lemma 5 is the reason why $\hat{q}_G = \arg\min_{q_G} \boldsymbol{L}_\lambda(q_G, \mu)$ can be computed in a distributed way. Indeed from $\partial \boldsymbol{L}_\lambda / \partial q_G = 0$ we get

$$X_{GG}^I \hat{q}_G + \frac{\partial v_G}{\partial q_G}(\lambda_{\max,G} - \lambda_{\min,G}) + \mu_{\max,G} - \mu_{\min,G} = 0.$$

By using (7), and by left-multiplying by $G = \left(X_{GG}^I\right)^{-1}$, we have

$$\hat{q}_G + \lambda_{\max,G} - \lambda_{\min,G} + G\,(\mu_{\max,G} - \mu_{\min,G}) = 0.$$

Therefore, the terms $\hat{q}_h$ in (27) corresponds element-wise to the $\arg\min_{q_G} \boldsymbol{L}_\lambda(q_G, \mu)$ in the linearized grid model, and a generally good approximation otherwise.

Remark 4. The proposed DVS deals with both constraints on v_G and on q_G. The voltage constraints may be violated during the iterations of the algorithm, but they are eventually satisfied. Instead, the reactive power constraints are treated as saturation constraints: thanks to the projection step in (28), they are guaranteed to be satisfied at any time t.

Remark 5. In the proposed DVS we have adopted a particular quadratic cost of the reactive power injections, described by the matrix X_{GG}^I. A discussion on the different options in terms of cost function goes beyond the scope of this paper, as the analysis is focused on whether the different strategies are capable of driving the systems to a feasible reactive power injection (i.e., to the set $\mathcal{F}$) or not. However, it is worth noticing that, in the linearized model, $X_{GG}^I q_G$ is the voltage drop caused by the reactive power injected by the microgenerators, which we call δv_G. From this point of view, the cost function (24a) can be rewritten as

$$\delta v_G^{\mathsf{T}} G \delta v_G.$$

Given that G is a Laplacian, this cost function promotes, among feasible reactive power injections, those that cause uniform voltage drops. Adopting a different cost function can, in general, require the measurement and exchange of other quantities. In [13], for example, a distributed strategy has been proposed to minimize power distribution losses, assuming that microgenerators can also measure voltage angles θ_h.

B. Convergence analysis

In this section we provide some insight on the convergence properties of the proposed DVS. The theoretical analysis in this section relies on the following two assumptions.

First, we assume that the inner iterations in step 1) of the algorithm reach their steady state before executing step 2). In fact, if the parameter K is chosen sufficiently large, these iterations will converge arbitrarily close to the solution of the the optimization problem in (25), and therefore

$$q_h(t) = [\hat{q}_h(t)]_{q_{\min,h}}^{q_{\max,h}} \approx \hat{q}_h(t) \approx q_G^* \tag{29}$$

where q_G^* is the solution of (25). The fact that $q_h(t)$ is in general different from q_G^* makes step 1) an *approximate* primal optimization step in the DVS algorithm. It is worth mentioning that when the parameter K is chosen sufficiently large, the size of this approximation error can be made arbitrarily small, and ultimately negligible. This has been confirmed in a number of numerical simulations, including the numerical examples in Section VI, and even in a preliminary experimental implementation, providing compelling evidence that the design of a "large enough" parameter K is typically easy. In the rest of the paper, we will assume that (29) holds as an equality.

The second assumption is the linearized grid model (7). In fact, based on the linear form of $v_G(q_G)$, the optimization problem (24) is a quadratic program with linear constraints. Assuming that its feasible space has a non-empty interior, this implies strong duality (via Slater constraint qualification [43]) and that both the optimization problem in (25) and the optimization program in (26) have a unique solution. Therefore, via [43, Proposition 6.1.1], both the dual functions $g(\lambda)$ and $g_\lambda(\mu)$ are continuously differentiable, and their subgradients are singletons.

Under these assumptions, both the iterations 1)-2)-3)-4) and the inner steps 1.1)-1.2)-1.3) are standard gradient ascent algorithms for the corresponding dual problems, and their convergence directly follow from [43, Proposition 1.2.3] under the conditions

$$0 < \alpha < \frac{2}{L} \quad \text{and} \quad 0 < \gamma < \frac{2}{L_\lambda},$$

where L and L_λ are two positive constants that satisfy respectively

$$\|\nabla g(\lambda) - \nabla g(\lambda')\| \leq L\|\lambda - \lambda'\|$$
$$\|\nabla g_\lambda(\mu) - \nabla g_\lambda(\mu')\| \leq L_\lambda\|\mu - \mu'\|.$$

While the step size α used in the update step 3) can be safely chosen to be sufficiently small, the step size γ should be selected in a way to guarantee a fast convergence rate of the iterations in step 1), in order to yield a close-to-optimal

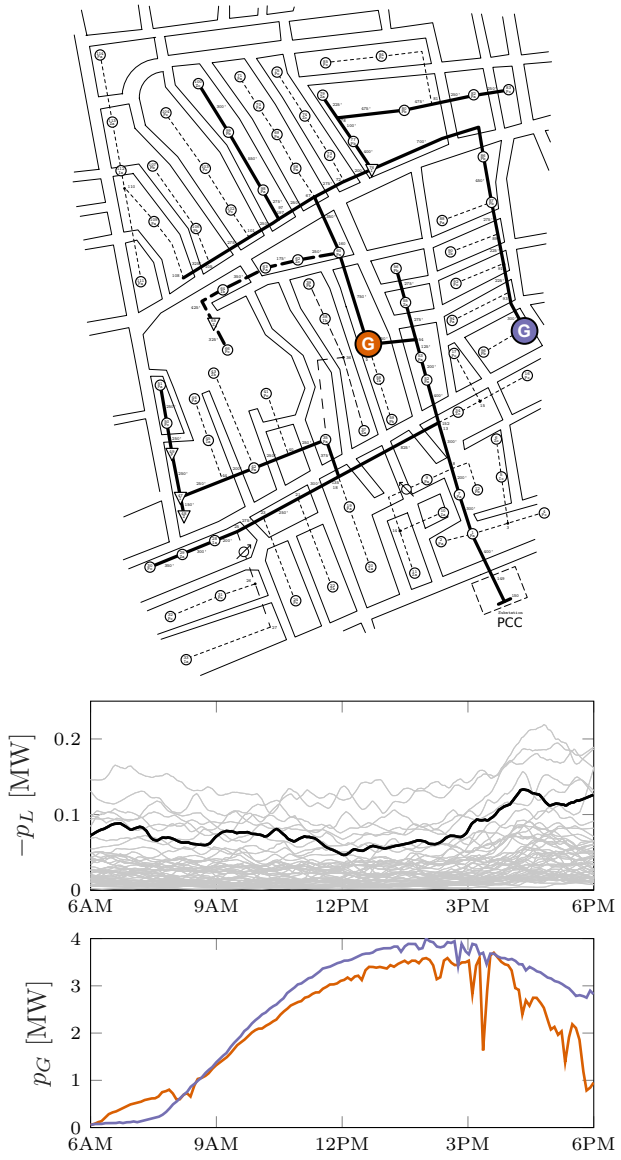

Figure 3. The IEEE 123-bus test feeder. The three-phase backbone that has been considered in the simulations is marked as a thick line. The substations is marked as PCC (point of common coupling). Two nodes host a microgenerator each, both capable also of injecting reactive power in order to support the feeder voltage profile. The load profiles and the generation profiles over 12 hours are plotted. The color code (purple and orange) is consistent across the next figures.

solution in K steps. In order to facilitate that, we explicitly compute an upper bound for the feasible value of γ.

Proposition 6. *Consider the optimization problem in* (25)*. The trajectory $\tau \to \hat{q}_G(\tau)$ generated by the iterations B.1-2-3 of the DVS algorithm converges to the optimal solution q_G^* for $\tau \to \infty$ if*

$$\gamma < \frac{1}{\rho(G)},$$

where ρ indicates the spectral radius.

VI. Simulations

In order to illustrate the practical significance of these results and their robustness with respect to both the unmodeled grid nonlinearities and the actuation delays, we simulated the behavior of different voltage control strategies on a quasi-stationary nonlinear AC power flow model.

As a testbed, we adopted the test feeder proposed in [41] and consisting in the three-phase backbone of the standard IEEE 123 distribution test feeder [44]. It is schematically reported in Figure 3. The power demand of each bus has been obtained by aggregating the power demand profiles available in the DiSC simulation framework [45]. They represent the power consumption of about 1200 individual households from the area around the Danish city Horsens, obtained as anonymized data from the Danish DSO NRGi. The resulting power demand profiles for a 12-hour period (6 AM to 6 PM) have been plotted in Figure 3, where one profile has been highlighted as an example. Two microgenerators have been added to the grid, in order to recreate the configuration used in Section IV-A. They correspond to two photovoltaic units, and their generation over the same 12-hour period is also reported in Figure 3.

The code used in this simulations is available online [46], [47].

The resulting overvoltage contingency is illustrated in the **Uncontrolled** panel of Figure 4. The two generators inject active power with unitary power factor, i.e. with zero reactive power, although they have a reactive power capability of 1 MVAR and 200 KVAR, respectively. In multiple buses, the voltage magnitude exceeds the limit of 1.05 p.u.

In the panel **Fully decentralized control (static)**, we simulate the effect of a purely local feedback law like the one proposed in [5], [7], [26], [27] and schematically represented in the left panel of Figure 1. We assumed a deadband for the voltages $[0.99, 1.01]$ p.u. For this and for the following control strategies, we assumed a sampling time of 5 seconds. This family of local static feedback strategies results in voltage violation at some buses, including one of the generator buses.

In the panel **Fully decentralized control (incremental)**, we simulate the effect of the purely local incremental feedback proposed in [21] and schematically depicted in the right panel of Figure 1. This approach does not strictly belong to the class of local strategies defined in Section IV. However, also in this case, voltages are not regulated below the overvoltage limit, and therefore this numerical experiments demonstrates the ineffectiveness of this fully decentralized control strategy.

In the panel **Networked control (DVS)** of Figure 4, we simulate the strategy that we proposed in Section V, which makes use of communication between the two microgenerators. We assume a ratio $K = 10$ between the sampling times of the fast and the slow part of the control law, and we allowed a time delay of 5 seconds between the update of set-points and the steady state of the voltages. We selected $\alpha = 10$ and $\gamma = 1/(2\rho(G))$, therefore satisfying the conditions for convergence that we derived in Section V-B. Via this coordination strategy, both agents successfully participate in the regulation of the voltage (even if one of the two measures a feasible voltage magnitude).

The convergence analysis of the networked control strategy in Section V-B relies on the approximation (29). In other words, it assumes that the variable $\hat{q}_G$ has converged to the solution q_G^* of (25) in K iterations. In order to verify this

assumption, we considered the same simulation as in Figure 4, and we zoom in on a time interval in which the system was subject to a significant disturbance of the generated active power. For that time interval, we plot both $\hat{q}_G$ and q_G^* in Figure 5. It is possible to see that because of the finite number of iterations that are completed at every step, $\hat{q}_G$ does not converge exactly to the minimizer q_G^*. It gets however extremely close, also because the internal variables $\mu_{\min,h}$ and $\mu_{\max,h}$ used in the iterations B.1-2-3 maintain their value when the "slower" variables $\lambda_{\min,h}$ and $\lambda_{\max,h}$ are updated (they are, in some sense, *warm-started*).

The difference between $\hat{q}_G(t)$ and q_G^* depends on both K and the number of microgenerators, as the size of the communication graph affects the convergence time. We repeated the same simulations adding increasingly many microgenerators with no active power injection, and no reactive power capabilities. These extra microgenerators do not affect the optimal solution of the problem, but they affect the communication graph and therefore the convergence time for dual problem. The worst case error for different values of N and K have been reported in the table in Figure 6.

The overall behavior of the algorithm seems very robust with respect to approximations in the dual optimization step. The bottom panels in Figure 6 show the voltage profile and the reactive power profile (together with the optimal reactive power profile q_G^*) for the case of $N = 48$ microgenerators and $K = 5$. Although the error $\hat{q}_G - q_G^*$ is significant, the resulting perturbation on the voltage profiles is tolerable.

VII. Conclusions

We first introduced a very general class of purely local control strategies and demonstrated via a counter-example that all the strategies in that class fail to drive the grid to a configuration of feasible voltages. Numerical simulations on a standard IEEE test case with real data show that this optimality gap can be easily observed in practice and that the phenomenon persists even when accounting for the nonlinearity of the power flow equations. By proposing both an analytical counter-example and an openly-accessible numerical testbed [46], we provided a simple yet effective benchmark that researchers and practitioners can use to validate their Volt/VAR control strategies.

In order to shed light on the crucial role of communication between microgenerators, we then proposed a distributed voltage control strategy that relies on precisely the same measurements and is capable of driving the system to the desired feasible region, as shown both in the convergence analysis and in simulations.

Essentially, this paper illustrates the potential of networked control solutions for this application. These solutions benefit from the advantage of being feedback strategies (robustness to model mismatch, rejection of disturbance, dynamic responsiveness, minimal computational effort). They can guarantee optimal voltage regulation similar to a centralized optimization-based approach, but compared to those they do not require full-state measurements, they allow seamless insertion and removal of agents (plug-and-play), and they do not assume the availability of the entire grid model at a single location (leader-less). These points are summarized in the following table.

	Control strategy		
	OPF	Networked	Decentralized
Feedback	✗	✓	✓
Leader-less	✗	✓	✓
Plug-and-play	✗	✓	✓
Low computation effort	✗	✓	✓
Communication	✓	✓	✗
Full-state measurement	✓	✗	✗
Optimal regulation	✓	✓ Sect. V-B	✗ Sect. IV-A

Appendix

Proof of Lemma 1

The statement can be proved by inspection, plugging (5) into (3), together with

$$\theta \approx \operatorname{Im} Xp - \operatorname{Re} Xq,$$

and using the first of the properties (4) of X expressed in rectangular coordinates, i.e.

$$\begin{cases} \operatorname{Re} Y \operatorname{Re} X - \operatorname{Im} Y \operatorname{Im} X = I - e_1 \mathbf{1}^\intercal \\ \operatorname{Im} Y \operatorname{Re} X + \operatorname{Re} Y \operatorname{Im} X = 0. \end{cases}$$

□

A. Proof of Proposition 2

Let us define the function

$$h(q, v) := g_h(q, v) - q.$$

It is a continuous function, such that for every v

$$h(q_{\min}, v) = g_h(q_{\min}, v) - q_{\min} \geq 0$$
$$h(q_{\max}, v) = g_h(q_{\max}, v) - q_{\max} \leq 0$$

Fix $v \in \mathbb{R}_{\geq 0}$. Furthermore, $h(\cdot, v)$ is a strictly decreasing function. In fact, if we consider $q_1 > q_2$, we have that

$$h(q_1, v) - h(q_2, v) = g_h(q_1, v) - g_h(q_2, v) - q_1 + q_2 < 0$$

Thus, there exists a unique configuration q such that $h(q, v) = 0$, i.e. $g_h(q, v) = q$. □

Proof of Proposition 3

Let $v, v' \in \mathbb{R}_{\geq 0}, v > v'$, and let $q = F_h(v), q' = F_h(v')$. To prove that $F_h(v)$ is weakly decreasing, let us assume that $q > q'$. Then, being $g_h(q, \cdot)$ a non-increasing function,

$$\begin{aligned} q' &< g_h(q, v') + q' - q \\ &\leq g_h(q, v) + q' - q = q' \end{aligned}$$

which is absurd.

Standard analysis results state that a non-increasing function whose image is a connected set is continuous. Thus, in order to prove the continuity, we just need to prove that the image of $F(v)$ is a connected set. To this aim, consider $v, v' \in \mathbb{R}_{\geq 0}, v >$

v' and $q = F_h(v), q' = F_h(v'), q \leq q'$. For every $q' < q'' < q$, from equation (12), we have that

$$g_h(q'', v) < g_h(q, v) + q'' - q = q'' \tag{30}$$

$$g_h(q'', v') > g_h(q', v') + q'' - q' = q'' \tag{31}$$

Since $g_h(q'', \cdot)$ is a continuous function, there exists $v' \leq v'' \leq v$ such that $g_h(q'', v'') = q''$, and thus q'' belongs to the image of $F(v)$. □

Proof of Proposition 6

Let us rewrite (25) as

$$\begin{aligned} \min_{q_G} \quad & \boldsymbol{L}(q_G, \lambda) \\ \text{subject to} \quad & \Phi q_G \leq b \end{aligned} \tag{32}$$

where

$$\Phi = \begin{bmatrix} I \\ -I \end{bmatrix}, \quad b = \begin{bmatrix} q_{\max,G} \\ -q_{\min,G} \end{bmatrix}.$$

Let us also rewrite the dual $g_\lambda(\mu)$ of this problem as

$$g_\lambda(\mu) = \boldsymbol{L}_\lambda(\hat{q}_G, \mu) \tag{33}$$

where $\hat{q}_G = \arg\min_{q_G} \boldsymbol{L}_\lambda(q_G, \mu)$ and

$$\boldsymbol{L}_\lambda(q_G, \mu) = \boldsymbol{L}(q_G, \lambda) + \mu^T(\Phi q_G - b). \tag{34}$$

Notice that because this latter problem is an unconstrained convex quadratic program, $\hat{q}_G$ is a continuously differentiable function of μ, with gradient $\nabla \hat{q}_G$. Moreover, $\hat{q}_G$ needs to satisfy

$$\nabla_{q_G} \boldsymbol{L}_\lambda(\hat{q}_G, \mu) = 0, \tag{35}$$

or equivalently

$$\nabla_{q_G} \boldsymbol{L}(\hat{q}_G, \lambda) + \mu\Phi = 0. \tag{36}$$

Let us compute the Hessian of $g_\lambda(\mu)$ by differentiating (33) twice. We first get

$$\nabla g_\lambda(\mu) = \nabla \hat{q}_G \nabla_{q_G} \boldsymbol{L}_\lambda(\hat{q}_G, \mu) + \Phi \hat{q}_G - b,$$

and, via (35),

$$\nabla g_\lambda(\mu) = \Phi \hat{q}_G - b.$$

By differentiating with respect to μ we obtain

$$\nabla^2 g_\lambda(\mu) = \nabla \hat{q}_G \Phi. \tag{37}$$

By differentiating (36) with respect to μ we get

$$\nabla \hat{q}_G \nabla^2_{q_G q_G} \boldsymbol{L}(\hat{q}_G, \lambda) + \Phi = 0$$

which implies

$$\nabla \hat{q}_G = -\Phi \left[\nabla^2_{q_G q_G} \boldsymbol{L}(\hat{q}_G, \lambda)\right]^{-1} = \Phi G. \tag{38}$$

Finally, by plugging (38) into (37) we obtain

$$\nabla^2 g_\lambda(\mu) = \Phi G \Phi.$$

A standard application of the mean value theorem allows to conclude that

$$\|\nabla g_\lambda(\mu) - \nabla g_\lambda(\mu')\| \leq \rho(\Phi G \Phi)\|\mu - \mu'\|$$

and consequently, via [43, Proposition 1.2.3], that the trajectory $\hat{q}_G(\tau)$ converges for any $\gamma < 2/\rho(\Phi G \Phi) = 1/\rho(G)$ (where in the last equality we used the fact that $\Phi G \Phi = \left[\begin{smallmatrix} 1 & -1 \\ -1 & 1 \end{smallmatrix}\right] \odot G$ and the properties of the Kronecker product [48, Theorem 4.2.12] to show that $\rho(\Phi G \Phi) = 2\rho(G)$). □

REFERENCES

[1] H. Farhangi, "The path of the smart grid," *IEEE Power Energy Mag.*, vol. 8, no. 1, pp. 18–28, Jan.-Feb. 2010.

[2] K. Clement-Nyns, E. Haesen, and J. Driesen, "The impact of charging plug-in hybrid electric vehicles on a residential distribution grid," *IEEE Trans. Power Syst.*, vol. 25, no. 1, pp. 371–380, Feb. 2010.

[3] J. A. P. Lopes, F. J. Soares, and P. M. R. Almeida, "Integration of electric vehicles in the electric power system," *Proc. IEEE*, vol. 99, no. 1, pp. 168–183, Jan. 2011.

[4] R. Tonkoski, L. A. C. Lopes, and T. H. M. El-Fouly, "Coordinated active power curtailment of grid connected PV inverters for overvoltage prevention," *IEEE Trans. Sustain. Energy*, vol. 2, no. 2, pp. 139–147, Apr. 2010.

[5] K. Turitsyn, P. Šulc, S. Backhaus, and M. Chertkov, "Options for control of reactive power by distributed photovoltaic generators," *Proc. IEEE*, vol. 99, no. 6, pp. 1063–1073, Jun. 2011.

[6] D. K. Molzahn, F. Dörfler, H. Sandberg, S. H. Low, S. Chakrabarti, R. Baldick, and J. Lavaei, "A survey of distributed optimization and control algorithms for electric power systems," *IEEE Trans. Smart Grid*, vol. 8, no. 6, pp. 2941–2962, Nov. 2017.

[7] P. Jahangiri and D. C. Aliprantis, "Distributed Volt/VAr control by PV inverters," *IEEE Trans. Power Syst.*, vol. 28, no. 3, pp. 3429–3439, Aug. 2013.

[8] K. Tanaka, M. Oshiro, S. Toma, A. Yona, T. Senjyu, T. Funabashi, and C. Kim, "Decentralised control of voltage in distribution systems by distributed generators," *IET Generation, Transmission Distribution*, vol. 4, no. 11, pp. 1251–1260, Nov. 2010.

[9] S. Karagiannopoulos, P. Aristidou, and G. Hug, "Data-driven local control design for active distribution grids using off-line optimal power flow and machine learning techniques," *IEEE Trans. Smart Grid*, 2019, to appear (Early Access).

[10] S. Kundu, S. Backhaus, and I. A. Hiskens, "Distributed control of reactive power from photovoltaic inverters," in *IEEE Int. Symp. Circuits Syst.*, 2013.

[11] H.-G. Yeh, D. F. Gayme, and S. H. Low, "Adaptive VAR control for distribution circuits with photovoltaic generators," *IEEE Trans. Power Syst.*, vol. 27, no. 3, pp. 1656–1663, Aug. 2012.

[12] A. Samadi, R. Eriksson, L. Söder, B. G. Rawn, and J. C. Boemer, "Coordinated active power-dependent voltage regulation in distribution grids with PV systems," *IEEE Trans. Power Del.*, vol. 29, no. 3, pp. 1454–1464, Jun. 2014.

[13] G. Cavraro and R. Carli, "Local and distributed voltage control algorithms in distribution networks," *IEEE Trans. Power Syst.*, vol. 33, no. 2, pp. 1420–1430, Mar. 2018.

[14] M. Farivar, X. Zhou, and L. Chen, "Local voltage control in distribution systems: An incremental control algorithm," *IEEE Int. Conf. Smart Grid Commun. (SmartGridComm)*, 2015.

[15] J. W. Simpson-Porco, F. Dörfler, and F. Bullo, "Voltage stabilization in microgrids via quadratic droop control," *IEEE Trans. Autom. Control*, vol. 62, no. 3, pp. 1239–1253, Mar. 2017.

[16] B. Zhang, A. D. Dominguez-Garcia, and D. Tse, "A local control approach to voltage regulation in distribution networks," in *Proc. North Amer. Power Symp. (NAPS)*, Sep. 2013.

[17] V. Kekatos, L. Zhang, G. B. Giannakis, and R. Baldick, "Fast localized voltage regulation in single-phase distribution grids," in *Proc. Intl. Conf. IEEE Smart Grid Communications*, 2015.

[18] H. Zhu and H. J. Liu, "Fast local voltage control under limited reactive power: Optimality and stability analysis," *IEEE Trans. Power Syst.*, vol. 31, no. 5, pp. 3794–3803, Sep. 2016.

[19] H. J. Liu, W. Shi, and H. Zhu, "Decentralized dynamic optimization for power network voltage control," *IEEE Trans. Signal Inf. Process. Netw.*, vol. 3, no. 3, pp. 568–579, Sep. 2017.

[20] X. Zhou, M. Farivar, and L. Chen, "Pseudo-gradient based local voltage control in distribution networks," in *Proc. 53rd Annu. Allerton Conf. Commun. Control Computing*, 2015, pp. 173–180.

[21] N. Li, G. Qu, and M. Dahleh, "Real-time decentralized voltage control in distribution networks," in *Proc. 52nd Annu. Allerton Conf. Commun. Control Computing*, 2014.

[22] X. Zhou and L. Chen, "An incremental local algorithm for better voltage control in distribution networks," in *Proc. 55th IEEE Conf. Decision Control (CDC)*, 2016.

[23] P. Nahata, S. Mastellone, and F. Dörfler, "Decentralized optimal projected control of PV inverters in residential microgrids," in *Proc. IFAC World Congr.*, 2017.

[24] DKE, "VDE-AR-N 4105: Generators connected to the LV distribution network - technical requirements for the connection to and parallel operation with low-voltage distribution networks," Tech. Rep., 2011.

[25] ENTSO-E Standard Draft, "Draft network code for requirements for grid connection applicable to all generators," Tech. Rep., 2012.

[26] IEEE Std 1547-2018, "Standard for interconnection and interoperability of distributed energy resources with associated electric power systems interfaces," IEEE, Standard, 2018.

[27] P. N. Vovos, A. E. Kiprakis, A. R. Wallace, and G. P. Harrison, "Centralized and distributed voltage control: impact on distributed generation penetration," *IEEE Trans. Power Syst.*, vol. 22, no. 1, pp. 476–483, Feb. 2007.

[28] R. Caldon, M. Coppo, and R. Turri, "Coordinated voltage control in MV and LV distribution networks with inverter-interfaced users," in *Proc. PowerTech*, 2013.

[29] S. Bolognani and S. Zampieri, "A distributed control strategy for reactive power compensation in smart microgrids," *IEEE Trans. Autom. Control*, vol. 58, no. 11, pp. 2818–2833, Nov. 2013.

[30] S. Bolognani, R. Carli, G. Cavraro, and S. Zampieri, "Distributed reactive power feedback control for voltage regulation and loss minimization," *IEEE Trans. Autom. Control*, vol. 60, no. 4, pp. 966–981, April 2015.

[31] F. Olivier, P. Aristidou, D. Ernst, and T. V. Cutsem, "Active management of low-voltage networks for mitigating overvoltages due to photovoltaic units," *IEEE Trans. Smart Grid*, vol. 7, no. 2, pp. 926–936, Mar. 2016.

[32] G. Cavraro, S. Bolognani, R. Carli, and S. Zampieri, "The value of communication in the voltage regulation problem," in *Proc. 55th IEEE Conf. Decision Control (CDC)*, 2016.

[33] M. Farivar, L. Chen, and S. Low, "Equilibrium and dynamics of local voltage control in distribution systems," in *Proc. 52nd IEEE Conference on Decision and Control*, 2013.

[34] E. Dall'Anese, H. Zhu, and G. B. Giannakis, "Distributed optimal power flow for smart microgrids," *IEEE Trans. Smart Grid*, vol. 4, no. 3, pp. 1464–1475, Sep. 2013.

[35] P. Šulc, S. Backhaus, and M. Chertkov, "Optimal distributed control of reactive power via the alternating direction method of multipliers," *IEEE Trans. Energy Convers.*, vol. 29, no. 4, pp. 968–977, Dec. 2014.

[36] B. Zhang, A. Y. S. Lam, A. D. Domínguez-García, and D. Tse, "An optimal and distributed method for voltage regulation in power distribution systems," *IEEE Trans. Power Syst.*, vol. 30, no. 4, pp. 1714–1726, Jul. 2015.

[37] B. A. Robbins and A. D. Domínguez-García, "Optimal reactive power dispatch for voltage regulation in unbalanced distribution systems," *IEEE Trans. Power Syst.*, vol. 31, no. 4, pp. 2903–2913, Jul. 2016.

[38] H. J. Liu, W. Shi, and H. Zhu, "Distributed voltage control in distribution networks: Online and robust implementations," *IEEE Trans. Smart Grid*, vol. 9, no. 6, pp. 6106–6117, Nov. 2018.

[39] G. Qu and N. Li, "Optimal distributed feedback voltage control under limited reactive power," *arXiv:1810.11121v2 [math.OC]*, Apr. 2019.

[40] S. Bolognani and F. Dörfler, "Fast power system analysis via implicit linearization of the power flow manifold," in *Proc. 53rd Annu. Allerton Conf. Commun. Control Computing*, 2015.

[41] S. Bolognani and S. Zampieri, "On the existence and linear approximation of the power flow solution in power distribution networks," *IEEE Trans. Power Syst.*, vol. 31, no. 1, 2016.

[42] I. W. Sandberg and A. N. Willson, "Some theorems on properties of DC equations of nonlinear networks," *The Bell System Technical Journal*, vol. 48, no. 1, pp. 1–34, Jan 1969.

[43] D. P. Bertsekas, *Nonlinear programming*, 2nd ed. Belmont (MA): Athena Scientific, 1999.

[44] W. H. Kersting, "Radial distribution test feeders," in *IEEE Power Engineering Society Winter Meeting*, vol. 2, Jan. 2001, pp. 908–912.

[45] R. Pedersen, C. Sloth, G. B. Andresen, and R. Wisniewski, "DiSC: A simulation framework for distribution system voltage control," in *Proc. European Control Conference*, 2015.

[46] S. Bolognani, "networked-volt-var - A comparison of Volt/VAR feedback control laws: fully decentralized vs networked strategies," GitHub, 2018. [Online]. Available: https://github.com/saveriob/networked-volt-var

[47] S. Bolognani, R. Carli, G. Cavraro, and S. Zampieri, "On the need for communication for voltage regulation of power distribution grids [source code]," CodeOcean, May 2019. [Online]. Available: https://doi.org/10.24433/CO.8982151.v1

[48] R. A. Horn and C. R. Johnson, *Topics in Matrix Analysis*. Cambridge University Press, 1991.

Saverio Bolognani received the B.S. degree in Information Engineering, the M.S. degree in Automation Engineering, and the Ph.D. degree in Information Engineering from the University of Padova, Italy, in 2005, 2007, and 2011, respectively. In 2006-2007, he was a visiting graduate student at the University of California at San Diego. In 2013-2014 he was a Postdoctoral Associate at the Laboratory for Information and Decision Systems of the Massachusetts Institute of Technology in Cambridge (MA). He is currently a Senior Researcher at the Automatic Control Laboratory at ETH Zurich. His research interests include the application of networked control system theory to power systems, distributed control and optimization, and cyber-physical systems.

Ruggero Carli received the Laurea Degree in Computer Engineering and the Ph.D. degree in Information Engineering from the University of Padova, Italy, in 2004 and 2007, respectively. From 2008 through 2010, he was a Post-doctoral Fellow with the Department of Mechanical Engineering, University of California at Santa Barbara. He is currently an Associate Professor with the Department of Information Engineering of the University of Padova. His research interests include control theory and, in particular, control under communication constraints, cooperative control, and distributed estimation.

Guido Cavraro received the B.Sc. degree in Information Engineering, the M.Sc. degree in Automation Engineering, and the Ph.D. degree in Information Engineering from the University of Padova, Italy, in 2008, 2011, and 2015, respectively. In 2015 and 2016, he was a postdoctoral associate at Department of Information Engineering of the Univiveristy of Padova. From 2016 to 2018, he was a postdoctoral associate with the Bradley Department of Electrical and Computer Engineering of Virginia Tech, USA. Currently, he is a Research Engineer with the Power Systems Engineering Center at National Renewable Energy Laboratory, USA. His research interests include control, optimization, and identification applied to power systems and smart grids.

Sandro Zampieri Sandro Zampieri received the Laurea degree in Electrical Engineering and the Ph.D. degree in System Engineering from the University of Padova, Italy, in 1988 and 1993, respectively. Since 2002 he is Full Professor in Automatic Control at the Department of Information Engineering of the University of Padova. He has been the head of the Department of Information Engineering from 2014 until 2018. In 1991-92, 1993 and 1996 he was Visiting Scholar at Laboratory for Information and Decision Systems, MIT, Cambridge. He has held visiting positions also at the Department of Mathematics of the University of Groningen and at the Department of Mechanical Engineering of the University of California at Santa Barbara.

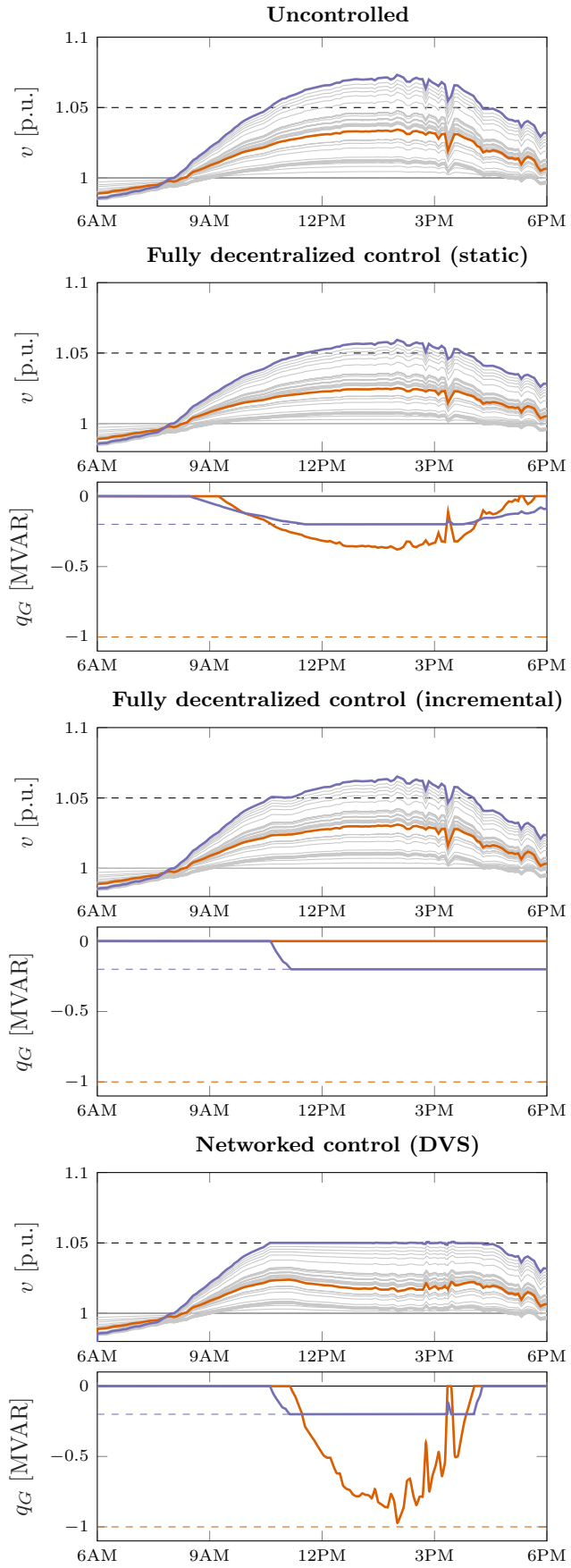

Figure 4. Comparison of different reactive power control strategies.

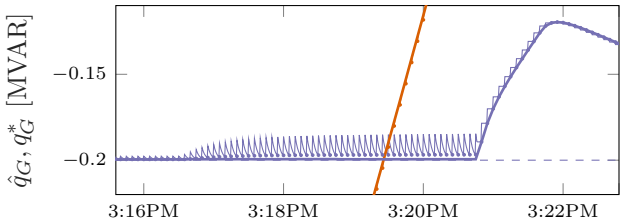

Figure 5. Detail of the difference between the approximate solution $\hat{q}_G$ to the dual optimization problem (25) (thin line) and the true solution q_G^* (thick line). Markers on the thin line represent the value of $\hat{q}_G$ at integer times.

Approximation error $\|\hat{q}_G(t) - q_G^*\|_\infty$ [MVAR]

	$K = 5$	$K = 10$	$K = 20$	$K = 40$
$N = 2$	1.3×10^{-2}	3.9×10^{-3}	5.9×10^{-4}	1.6×10^{-5}
$N = 3$	4.3×10^{-2}	1.9×10^{-2}	6.6×10^{-3}	1.5×10^{-3}
$N = 6$	2.5×10^{-1}	1.4×10^{-1}	7.0×10^{-2}	3.3×10^{-2}
$N = 12$	5.5×10^{-1}	4.2×10^{-1}	2.7×10^{-1}	1.1×10^{-1}
$N = 24$	6.9×10^{-1}	4.4×10^{-1}	5.0×10^{-1}	3.4×10^{-1}
$N = 48$	8.4×10^{-1}	4.4×10^{-1}	5.3×10^{-1}	3.9×10^{-1}

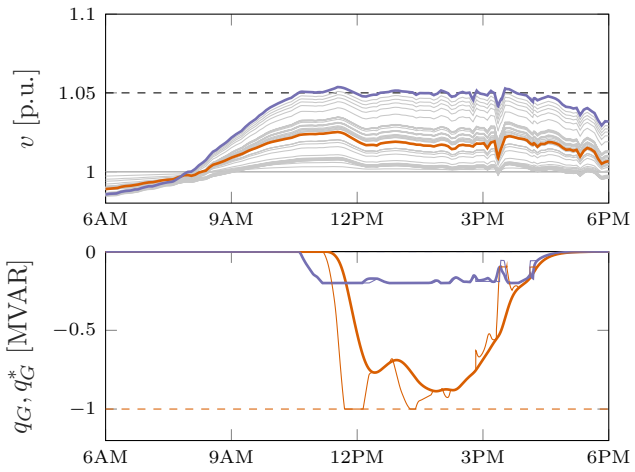

Figure 6. Analysis of the accuracy of the finite-time solution to the dual optimization problem (25) as a function of the number of generators N and the number of iterations K. The lower panel illustrates the case with the largest approximation error: $N = 48$, $K = 5$. The thick line represents the reactive power q_G, while the thin line represents the optimal solution q_G^*.